



Is the alumino-boron carbide Al₃BC a promising thermoelectric material? A computational exploration

A. Huguenot, A. Riot, B. Boucher, B. Fontaine, Stéphane Cordier, R. Al Rahal Al Orabi, H. Hillebrecht, T. Mori, J.-F. Halet, R. Gautier

► To cite this version:

A. Huguenot, A. Riot, B. Boucher, B. Fontaine, Stéphane Cordier, et al.. Is the alumino-boron carbide Al₃BC a promising thermoelectric material? A computational exploration. Solid State Sciences, 2020, 104, pp.106205. 10.1016/j.solidstatesciences.2020.106205 . hal-02569949

HAL Id: hal-02569949

<https://univ-rennes.hal.science/hal-02569949>

Submitted on 20 Oct 2021

HAL is a multi-disciplinary open access archive for the deposit and dissemination of scientific research documents, whether they are published or not. The documents may come from teaching and research institutions in France or abroad, or from public or private research centers.

L'archive ouverte pluridisciplinaire **HAL**, est destinée au dépôt et à la diffusion de documents scientifiques de niveau recherche, publiés ou non, émanant des établissements d'enseignement et de recherche français ou étrangers, des laboratoires publics ou privés.

Is the Alumino-boron Carbide Al_3BC a Promising Thermoelectric Material? A Computational Exploration.

Arthur Huguenot,¹ Aurélien Riot,¹ Benoît Boucher,¹ Bruno Fontaine,¹ Stéphane Cordier,¹ Rabih Al Rahal Al Orabi,² Harald Hillebrecht,³ Takao Mori,^{4,5} Jean-François Halet,^{1,a} and Régis Gautier^{1,a}

¹*Univ Rennes, Ecole Nationale Supérieure de Chimie de Rennes, CNRS, ISCR – UMR 6226, F-35000 Rennes, France*

²*Central Michigan University, Department of Physics, Mt. Pleasant, MI 48859, USA.*

³*Institut für Anorganische und Analytische Chemie, Albert-Ludwigs-Universität, Albertstraße 21, D-79104 Freiburg, Germany*

⁴*WPI International Center for Materials Nanoarchitechtonics (WPI-MANA) and Center for Functional Sensor & Actuator (CFSN), National Institute for Materials Science (NIMS), Namiki 1-1, Tsukuba 305-0044, Ibaraki, Japan*

⁵*Graduate School of Pure and Applied Sciences, University of Tsukuba, Tennoudai 1-1-1, Tsukuba 305-8671, Japan*

^aAuthors to whom correspondence should be addressed: halet@univ-rennes1.fr (J.-F. H), rgautier@ensc-rennes.fr (R. G.)

Abstract

The structural, electronic and vibrational properties of the ternary borocarbide Al_3BC are studied using first principles calculations in order to evaluate its potential use for thermoelectric applications. A fuller description of its crystal structure was achieved on the basis of an orthorhombic unit cell, twice larger than the previously reported experimental one. Using a semi-classical approach, the electronic transport properties were studied, and a high power factor is expected for this compound. A high thermal conductivity is foreseen on the basis of phonon calculations, suggesting that further developments aiming at its reduction would be necessary for thermoelectric applications.

1. Introduction

Boron is an element that shows a propensity to form diverse atomic network structures where clustering dominate. To a lesser extent, this is also the case for carbon, which has been much more extensively studied for compounds such as nanotubes, fullerenes, graphite-related materials... Interestingly, when boron and carbon elements are combined together in a more or less equal content with transition metals, they behave rather similarly leading to the formation of multinary boron carbide compounds. Boron-containing compounds are fascinating owing to their rich and varied structural chemistry and their fascinating physical properties [1,2,3]. This includes solid-state materials of formula M_xByC_z where M is a rare-earth metal, which exhibit a broad diversity of original architectures, often unique. The chemical bonding in most of these compounds can be rationalized by considering the interaction between main-group atoms first, and with the non-metal framework in a second step [4,5,6]. In these ternary borocarbides, the light elements can form either two-dimensional networks, which alternate with two-dimensional nets of metal atoms, or one-dimensional chains of boron and carbon atoms embedded in a metallic environment. Pseudo-molecules, from triatomic species to B_5C_8 finite chains, can also be drowned into a metallic matrix. Among these materials, Sc_2BC_2 , reported a while ago by Bauer and co-workers, is a unique compound where only BC_2 finite linear chains are present in the structure [7,8]. Later, Oeckler *et al.* synthesized the related compound Lu_3BC_3 that contains similar linear BC_2 units and additionally slabs of isolated carbon atoms in a metallic environment [9]. The electronic structure of both compounds is characterized by covalent bonding between the metallic matrix and the formally $(BC_2)^{5-}$ non-metal anions [10].

Ternary boron carbides are also encountered with aluminum. Indeed, a few aluminum-rich phases of the Al–B–C system have been investigated. For instance, the crystal structure of Al_3BC_3 was reported by Hillebrecht and Meyer [11]. It adopts a structure similar to that of Lu_3BC_3 , with linear BC_2 units and isolated carbon atoms. First-principles calculations showed that the covalent bonding in this compound is stronger than in the lutetium and scandium analogs [10]. Its low shear-strain resistance was theoretically studied [12]. Moreover, semiconducting properties are expected for Al_3BC_3 whereas metallic ones are envisioned for Lu_3BC_3 and Sc_2BC_2 . The ternary compound Al_3BC is another example of ternary alumino-boron carbide recently studied because of its chemical and thermal stabilities as well as its promising mechanical properties [13,14,15,16,17]. Al_3BC plays a part in the processing of B_4C –Al metal matrix composites that received considerable attention due to their superior thermal conductivity, light weight, promising tribological properties [18,19]. Al_3BC crystals were used

to reinforce aluminum-based alloys commonly used for automotive and aerospace applications [20]. Halverson *et al.* reported for the first time the synthesis of Al₃BC [21]. More than ten years later, Viala *et al.* [13] identified a hexagonal unit cell with $a = 3.491(2)$ Å and $c = 11.541(4)$ Å for this compound. In 1997, Meyer and Hillebrecht reported its crystal structure to be a closest packing of Al (sequence ABACBC) with alternating layers of trigonal bipyramids CAI₅ and edge-sharing BAI₆ octahedra, connected by common corners (Fig. 1) [14]. It is noteworthy to mention that anisotropic refinements and difference Fourier syntheses showed that Al₂ atom occupies a position disordered in the z -direction around the site $2b$ at $(0\ 0\ \frac{1}{4})$ (cf. Figure 1).

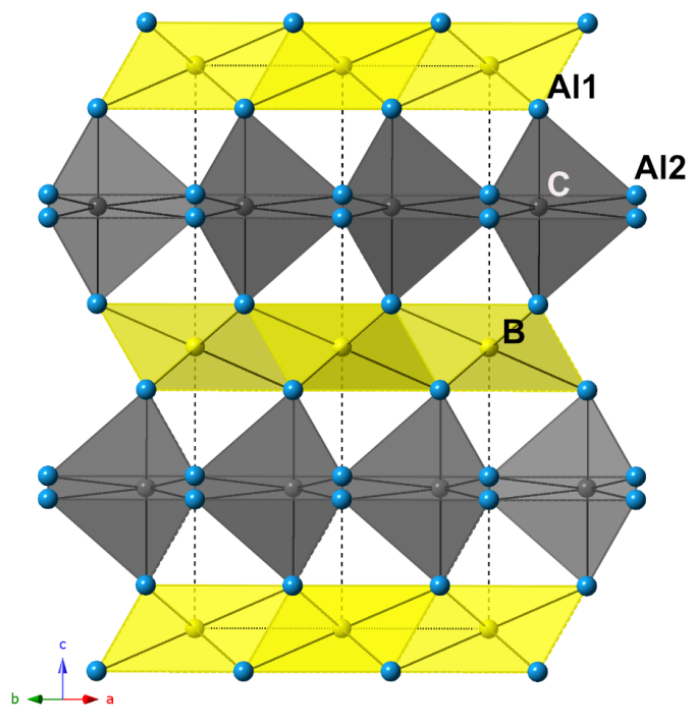


Fig. 1. Crystal structure of Al₃BC resulting from X-ray diffraction studies [14].

Several boron carbon materials have studied for their thermoelectric properties. The figure of merit ZT , which characterizes the thermoelectric efficiency of a material [22], of boron carbide reaches 1.06 at 1250 K for some samples of this material, demonstrating that it is a potential thermoelectric material for use at high temperatures [23]. Furthermore, boron cluster-containing compounds such as YB₆₆ and RB₄₄Si₂ (R = rare-earth) have generally been found to exhibit low thermal conductivity [24,25,26]. In all these materials, disorder from partial occupancy of the atomic sites seems to play a major part in their intrinsic low thermal conductivity.

The best thermoelectric candidates are highly doped semiconductors. According to their relative electronegativity, the following charge distribution can be proposed $(Al^{3+})_3(B^{5-})(C^{4-})$. This suggests semiconducting properties for Al_3BC . On the hypothesis of a modest thermal conductivity, this makes Al_3BC a material of interest for thermoelectric applications. In this manuscript, we theoretically analyze its electronic structure, electronic transport coefficients, and vibrational properties.

2. Computational Details

Geometry optimizations were performed using the VASP code [27] based on density functional theory (DFT) [28,29]. The exchange-correlation interaction was described within the generalized gradient approximation in the parametrization of the Perdew–Burke–Ernzerhof functional [30]. Projector-augmented wave potentials were used for all atoms [31]. Calculations were performed with a cut-off energy of 400 eV. The electronic wave functions were sampled on dense densities in the irreducible BZ using the Monkhorst method. Geometry optimizations including cell parameters and atomic positions were carried out without any symmetry constraints. To probe the dynamical stability of Al_3BC , theoretical phonon spectra were calculated based on the supercell approach using the PHONOPY package [32].

Electronic transport coefficients were calculated within the Boltzmann Transport Equation. A constant [relaxation time](#) τ for the electrons was assumed as well as a rigid band structure [33,34], as implemented in the BoltzTrap-1.2.5 code [35]. 10 000 k -points in the BZ were used to compute the band derivatives for transport calculations. Since pure DFT exchange–correlation functionals are known to underestimate experimental band gaps, the modified Becke–Johnson (mBJ) functional proposed by Blaha and Tran was used [36]. With a reduced computational cost, this functional yields band gaps with an accuracy similar [to GW](#) methods or hybrid functionals. The WIEN2k program package was used to perform this mBJ-DFT calculations [37]. This program is based on the linearized augmented plane wave + local orbital method where the unit cell is partitioned between spheres centered on the atomic sites and the interstitial region. Sphere sizes of 1.98, 1.90, and 1.79 bohr were used for Al, B, and C spheres, respectively. The charge density was expanded up to the reciprocal vector G_{\max} equal to 14 \AA^{-1} . Charge self-consistency was obtained from 120 irreducible k -points. Electronic dispersion curves were shifted to set the Fermi level to 0 eV arbitrarily.

Elastic properties calculations were carried out with the CASTEP 8.0 code [38] using the PBEsol functional [39]. All ultrasoft pseudopotentials were generated using OTF_ultrasoft-pseudopotential generator included in the program. The cutoff energy for plane-waves was set at 750 eV.

3. Results and Discussion

Structural Properties. In order to study the electronic structure of Al₃BC, a model crystal structure had to be considered since Al₂ atoms occupy a half-occupied position. Moreover, this disorder cannot be solved within the small unit cell and high symmetry proposed experimentally. In a first model, Al₂ atoms were located at (0 0 1/4) in order to consider the *P*6₃/mmc space group. In agreement with the formal charge distribution, the corresponding band structure suggests semiconducting properties with a band gap of *ca.* 1 eV (not shown here). However, computation of vibrational properties of this model showed imaginary frequencies of about 4.50i THz. The atom-projected vibration DOS sketched in Fig. 2 shows that Al atoms are mainly contributing to these imaginary frequencies. Going deeper in the analysis clearly shows that these imaginary frequencies are indeed mostly due to Al₂ atoms. Such computed vibrational properties are expected since this model simplifies the crystal structure resulting from X-ray diffractions studies. Consequently, symmetry constraints were suppressed during geometry optimizations. Since phonon calculations still showed negative frequencies associated with the same Al₂ atoms, larger unit cells were considered as well for the geometry optimizations. Finally, relaxation of cell parameters and atomic positions led to the crystal structure sketched in Fig. 3. This structure can be described with an orthorhombic unit cell with $a = 11.5480 \text{ \AA}$, $b = 3.4985 \text{ \AA}$, and $c = 6.0451 \text{ \AA}$ considering the *Pnma* space-group. [This unit cell is roughly twice bigger than the *P*6₃/mmc one](#). Atomic positions are given in Table 1. It is noteworthy to mention that no imaginary frequencies are computed for this structure (*vide infra*). As in the *P*6₃/mmc crystal structure, it is based on BA₆ octahedra that alternate with trigonal bipyramidal CA₅ polyhedra linked *via* common vertices. In the *Pnma* structure, the Al1-B and Al1'-B distances in the octahedra range from 2.187 Å to 2.225 Å (see Table 2). The average distance of the boron atom with vertices of the octahedra is slightly longer (2.209 Å) than the corresponding one in the *P*6₃/mmc structure (2.195 Å). Moreover, B-Al2 contacts equal to 2.473 Å are present in the *Pnma* structure whereas corresponding contacts are measured at 2.644 Å in the higher symmetry structure. In this latter, (Al₂)₃ triangles of the trigonal pyramids CA₅ are coplanar whereas they are tilted in the *Pnma* structure (cf. Fig. 3). It must be noted that the bonds of the C with the vertices of the trigonal bipyramids (Al1 and Al1' positions) are

no more parallel to the ones of the neighboring pyramids, and to the cell parameter as well. As Al-B distances, Al-C contacts in the bipyramidal polyhedra are computed slightly longer in the *Pnma* structure compared to the *P6₃/mmc* one resulting from X-ray diffraction studies. Such a difference may arise from the light overestimation of the cell parameters that is generally observed when PBE exchange-correlation functional is considered for the geometry optimization.

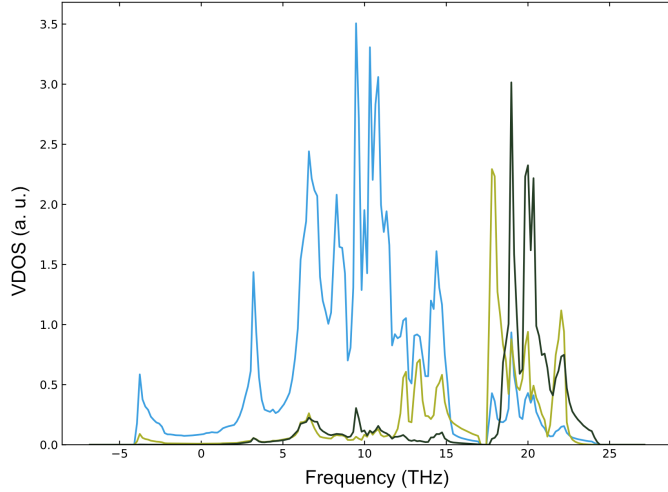


Fig. 2. Atom-projected vibrational DOS of Al_3BC with *P6₃/mmc* crystal structure: Al (blue), B (yellow) and C (grey) atomic projections.

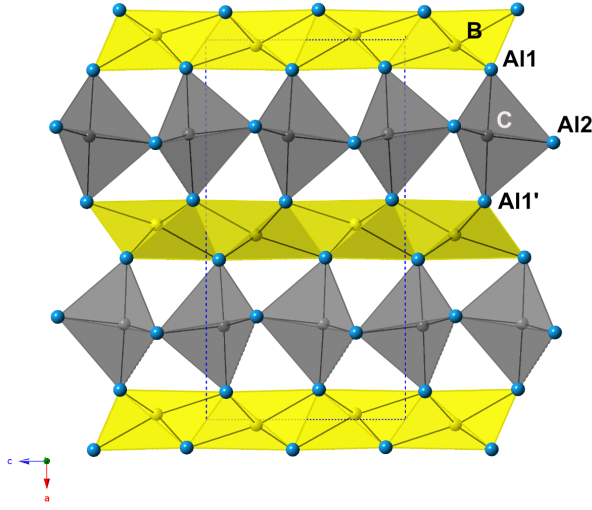


Fig. 3. *Pnma* crystal structure of Al_3BC resulting from DFT calculations. The unit cell is drawn with dotted blue lines.

Table 1. Atomic positions of Al₃BC computed in the *Pnma* space-group.

	<i>x / a</i>	<i>y / b</i>	<i>z / c</i>
Al1	0.4266	3/4	0.5994
Al1'	0.5790	3/4	0.9342
Al2	0.2716	3/4	0.2531
B	0.4858	3/4	0.2491
C	0.2526	3/4	0.5870

Table 2. Selected distances (Å) of Al₃BC crystal structures.

<i>P6₃/mmc</i> [14]			<i>Pnma</i>		
Al1 – C	2.002 (× 1)	Al1 – C	2.011 (× 1)		
B	2.195 (× 3)	B	2.219 (× 2) – 2.225 (× 1)		
Al1	2.670 (× 3)	Al1	2.716 (× 2)		
		Al1'	2.682 (× 1)		
Al2	2.677 (× 3)	Al2	2.755 (× 1) – 3.027 (× 2)		
		Al1' – C	2.009 (× 1)		
		B	2.187 (× 1) – 2.202 (× 2)		
		Al1	2.682 (× 1)		
		Al1'	2.650 (× 2)		
		Al2	2.705 (× 2) – 2.919 (× 1)		
Al2 – C	2.025 (× 3)	Al2 – C	2.031 (× 1) – 2.036 (× 2)		
Al1	2.672 (× 3)	B	2.473 (× 1)		
Al1	3.048 (× 3)	Al1	2.755 (× 1) – 3.027 (× 2)		
		Al1'	2.705 (× 2) – 2.919 (× 1)		
Al2	0.473				

Electronic properties. The band structure of Al₃BC with *Pnma* crystal structure sketched in Fig. 4, suggests semiconducting properties with a direct band gap of *ca.* 1.2 eV. Dispersive bands are computed in almost all directions suggesting good electrical conductivity for this compound upon doping. Atom-projected DOS curves in the range [-5, 5] eV (not shown here) indicate that all the atoms significantly contribute to the occupied bands and higher vacant

bands as well. This demonstrates the presence of strong covalent interactions in the structure. The top of the valence band is mainly based on B and Al1 atoms whereas all atoms equally contribute to the bottom of the conduction band.

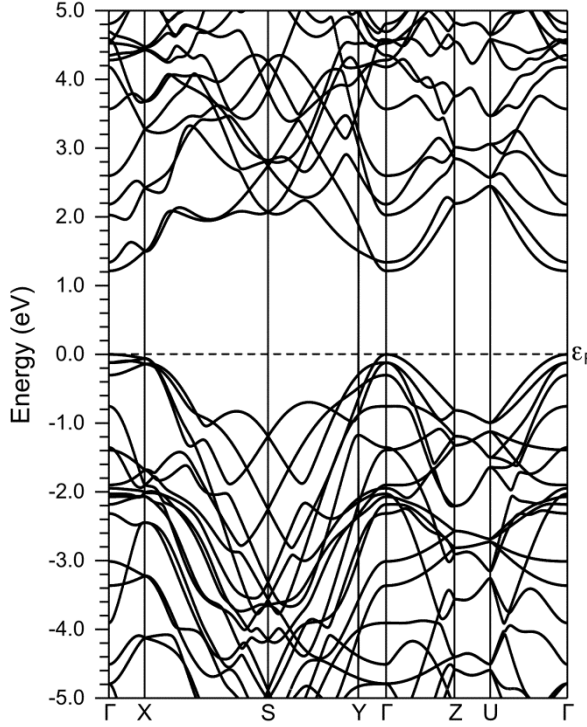


Fig. 4. Band structure of Al_3BC with *Pnma* crystal structure.

The electronic transport properties were computed for Al_3BC using the semi-classical approach (see computational details). This approach is based on the approximation of a constant relaxation time. Thus, the electrical conductivity can only be roughly predicted. On the contrary, the thermopower, which does not rely on the knowledge of the relaxation time, was computed as a function of the chemical potential. It is sketched in Fig. 5. At 300 K the maximum thermopower value is more than twice higher than that computed at 800 K. For both temperatures, the maximum thermopower value for *p*-type doping is similar to that obtained for *n*-type doping. At 300 K, absolute values larger than $1500 \mu\text{V K}^{-1}$ are computed. Such values make Al_3BC a promising material for thermoelectric applications. This is even more true that a good electrical conductivity [upon both *n*- and *p*-doping is also expected because of the dispersive character of the bands that lie in the vicinity of the Fermi level \(cf. Fig. 4\)](#).

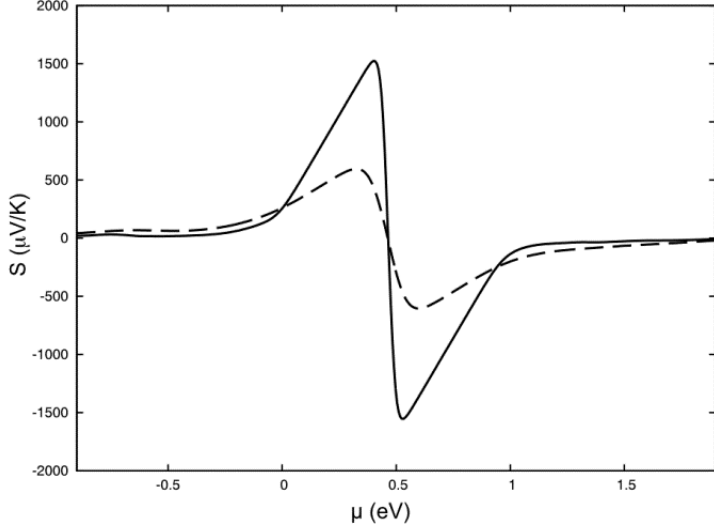


Fig. 5. Seebeck coefficient (S) computed as a function of the chemical potential (μ) for Al_3BC with $Pnma$ crystal structure at 300 K (plain) and 800 K (dotted).

Phonon and elastic properties. Figs. 6 and 7 display phonon dispersions and vibrational DOS, respectively, for Al_3BC . It is well known that the acoustic phonons are the most important ones for thermal transport because of their larger sound velocity. However, low optical modes constitute a possible source of scattering and should not be ignored [40,41,42]. Three acoustic modes have zone boundary frequencies around ~ 4.5 THz along the three crystal structure directions. As it can be seen from the vibrational DOS curves shown in Fig. 7, the acoustic and low optical modes frequencies are mainly dominated by Al atoms. However, these acoustic frequency modes values are much larger than those found in colusite [43,44], nitrides [45], or oxychalcogenides [46] for instance, which exhibit low thermal conductivity. Furthermore, all acoustic modes around the center of the BZ Γ are not soft, which will probably lead to high average sound velocities and high average Debye temperatures, resulting unfortunately in a (too) high thermal conductivity [47].

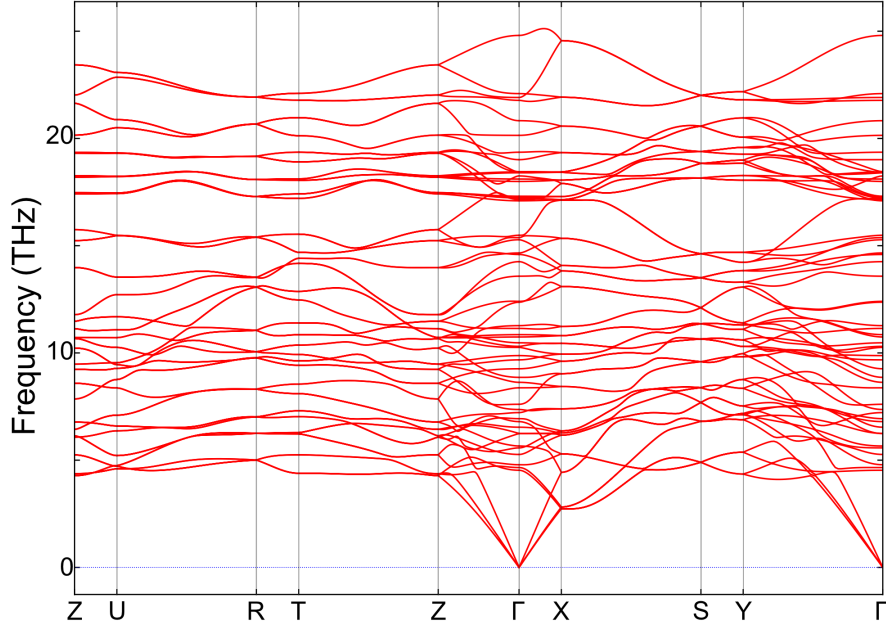


Fig. 6. Phonon dispersion for Al_3BC with *Pnma* crystal structure.

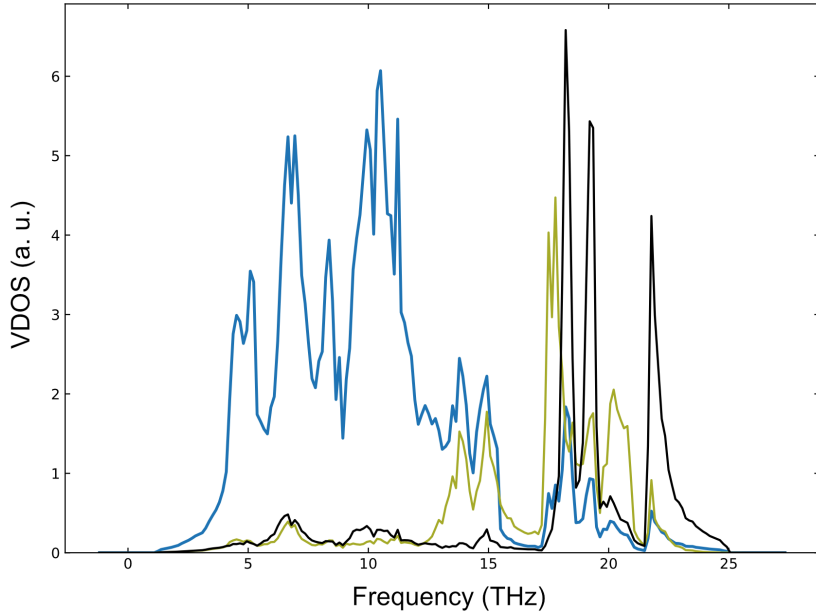


Fig. 7. Atom-projected vibrational DOS of Al_3BC with *Pnma* crystal structure: Al (blue), B (yellow) and C (grey) atomic projections.

In order to gain more information about the thermal conductivity of Al_3BC compound, the longitudinal (v_l) and transversal (v_t) phonon velocities, Young's moduli (E), Grüneisen parameters (γ) and Debye temperatures were computed from elastic properties calculations. As shown in Table 3, the average phonon velocity, Young's moduli, and Grüneisen parameters are 7269 ms^{-1} , 128 GPa , and 1.1 , respectively. Generally, large average phonon velocity, large

Young's modulus, and small Grüneisen parameters reflect strong interatomic bonding strength and weak anharmonicity in the crystal lattice, which result in rather important thermal conductivity [41].

Table 3. Calculated Young's modulus, longitudinal (v_l), transverse (v_t), and average (v_m) sound velocities, Grüneisen parameter (γ) and Debye temperature (θ_D) for Al_3BC .

E (GPa)	v_l ($m\ s^{-1}$)	v_t ($m\ s^{-1}$)	v_m ($m\ s^{-1}$)	γ	θ_D (K)
281	10212	6627	7261	1.1	940

Using Debye equation [48], the Debye temperature was calculated to be 940 K. Such a value is very high and should lead to a large thermal conductivity according to Slack's equation [49]. Indeed, the thermal conductivity is calculated to be around $40\ \text{W m}^{-1}\ \text{K}^{-1}$ for Al_3BC . Knowing that good thermoelectric materials have a thermal conductivity of the order of a couple of $\text{W m}^{-1}\ \text{K}^{-1}$, this value is very high for thermoelectric application requirement and may prevent the Al_3BC compound to be considered as a promising candidate for thermoelectric application. However, low frequencies modes are dominated by Al atoms as indicated by the VDOS. This may allow to tune the thermal conductivity further by doping Al by heavier elements such as In and/or Tl, and/or by reducing the grain size to enhance the boundary scattering of heat-carrying phonons or by enhancing structural disordering [50,51]

4. Conclusion

DFT calculations were carried out to study the structural, electronic and vibrational properties of the ternary aluminum boron carbide Al_3BC . Computation of phonon properties confirmed that a supercell has to be considered for a better description of its crystal structure. First-principles calculations demonstrated that an orthorhombic unit cell can be proposed for Al_3BC . The major difference of this *in silico* crystal structure with the previously reported one lies in the small tilting of the trigonal basis of the Al_5C bipyramids. Semiconducting properties are expected for this compound. Using a semi-classical approach, a high Seebeck coefficient is computed for this compound. Assuming a good electrical conductivity (owing to the dispersive nature of its band structure), a high-power factor is expected for this compound. However, calculations of phonon and elastic properties suggest a high thermal conductivity. This latter may be reduced by partial substitution of aluminum atoms in the structure by heavier elements or by nano-structuration. Furthermore, this material may also be considered as a promising

candidate for other applications such as thermal management in which a semiconductor with high thermal conductivity is required.

Among the rather long list of ternary boron carbides, which were reported, a few show some semiconducting properties and reasonable thermoelectric power. Results obtained here on Al₃BC are encouraging to theoretically investigate their thermoelectric properties.

Acknowledgements

A. H. and B. B. are indebted to the Région Bretagne for a PhD grant. These studies were facilitated within the scope of the France Japan International Collaboration Framework through the Laboratory for Innovative Key Materials and Structures (UMI 3629 LINK), financially supported by Saint-Gobain, Centre National de la Recherche Scientifique (CNRS), Université de Rennes 1 (UR1), and National Institute for Materials Science (NIMS).

References

- 1 T. Mori, Higher Borides in *Handbook on the Physics and Chemistry of Rare Earths* (Elsevier, 2008) pp. 105-173. [https://doi.org/10.1016/S0168-1273\(07\)38003-3](https://doi.org/10.1016/S0168-1273(07)38003-3)
- 2 S. Lassoued, R. Gautier, J.-F. Halet, The Electronic Properties of Metal Borides and Borocarbides: Differences and Similarities in *Boron Rich Solids: Sensors, Ultra High Temperature Ceramics, Thermoelectrics, Armor*, Eds. N. Orlovskaya, M. Lugovy (Springer Science and Business Media V. B., 2011) pp. 95-114. https://doi.org/10.1007/978-90-481-9818-4_7
- 3 B. Boucher, J.-F. Halet, Boron in Solid-state Chemistry: Some Portraits of Metal Borides Taken from a Rich Structural Gallery in *Handbook of Boron Science with Applications In Organometallics, Catalysis, Materials and Medicine*, Eds. N. Hosmane, R. Eagling, (World Science Publishers, London, 2019), pp. 159-188. https://doi.org/10.1142/9781786344663_0005
- 4 V. Babizhetkyy, J. Bauer, R. Gautier, K. Hiebl, A. Simon, J.-F. Halet, Structural, Electronic, and Physical Properties of Solid-State Rare-Earth Boride Carbides in *Handbook on the Physics and Chemistry of Rare Earths* (Elsevier, 2018) pp. 145-269. <http://dx.doi.org/10.1016/bs.hpcr.2018.05.001>
- 5 J. Bauer, J.-F. Halet, J.-Y. Saillard, Rare earth metal borocarbides: Examples of coordination compounds in solid-state chemistry, *Coord. Chem. Rev.* **178-179**, 723 (1998). [https://doi.org/10.1016/S0010-8545\(98\)00106-4](https://doi.org/10.1016/S0010-8545(98)00106-4)
- 6 M. Ben Yahia, J. Roger, X. Rocquefelte, R. Gautier, J. Bauer, R. Guérin, J.-Y. Saillard, J.-F. Halet, Portraits of some representatives of metal boride carbide and boride silicide compounds, *J. Solid State Chem.* **179**, 2779 (2006). <https://doi.org/10.1016/j.jssc.2005.12.032>
- 7 J.-F. Halet, J.-Y. Saillard, J. Bauer, Electronic structure of the new rare earth borocarbide Sc_2BC_2 , *J. Less-Comm. Metals* **158**, 239 (1990). [https://doi.org/10.1016/0022-5088\(90\)90059-S](https://doi.org/10.1016/0022-5088(90)90059-S)
- 8 Y. Shi, A. Leithe-Jasper, T. Tanaka, New Ternary Compounds $\text{Sc}_3\text{B}_{0.75}\text{C}_3$, $\text{Sc}_2\text{B}_{1.1}\text{C}_{3.2}$, $\text{ScB}_{15}\text{C}_{1.60}$ and Subsolidus Phase Relations in the Sc–B–C System at 1700°C, *J. Solid State Chem.* **148**, 250 (1999). <https://doi.org/10.1006/jssc.1999.8446>
- 9 O. Oeckler, C. Jardin, Hj. Mattausch, A. Simon, J.-F. Halet, J.-Y. Saillard, J. Bauer, Synthesis, Characterization, Structural and Theoretical Analysis of a New Rare-Earth Boride Carbide: Lu_3BC_3 , *Z. Anorg. Allg. Chem.* **627**, 1389 (2001). [https://doi.org/10.1002/1521-3749\(200106\)627:6<1389::AID-ZAAC1389>3.0.CO;2-G](https://doi.org/10.1002/1521-3749(200106)627:6<1389::AID-ZAAC1389>3.0.CO;2-G)
- 10 C. Jardin, H. Hillebrecht, J. Bauer, J.-F. Halet, J.-Y. Saillard, R. Gautier, First-principles study of ternary metal borocarbide compounds containing finite linear BC_2 units, *J. Solid State Chem.* **176**, 609 (2003). [https://doi.org/10.1016/S0022-4596\(03\)00348-7](https://doi.org/10.1016/S0022-4596(03)00348-7)

-
- 11 H. Hillebrecht, F. D. Meyer, Synthesis, Structure, and Vibrational Spectra of Al_3BC_3 , a Carbidecarboroborate of Aluminum with Linear ($\text{C}=\text{B}=\text{C}$)⁵⁻Anions, *Angew. Chem. Int. Ed. Engl.* 35, 2499 (1996). <https://doi.org/10.1002/anie.199624991>
- 12 J. Wang, Y. Zhou, T. Liao, Z. Lin, First-principles prediction of low shear-strain resistance of Al_3BC_3 : A metal borocarbide containing short linear BC_2 units, *Appl. Phys. Lett.* 89, 021917 (2006). <https://doi.org/10.1063/1.2220549>
- 13 J. C. Viala, J. Bouix, G. Gonzalez, C. Esnouf, Chemical reactivity of aluminium with boron carbide, *J. Mater. Sci.* 32, 4559 (1997). <https://doi.org/10.1023/A:101862540>
- 14 F. D. Meyer, H. Hillebrecht, Synthesis and crystal structure of Al_3BC , the first boridecarbide of aluminium, *J. Alloys Compd.* 252, 98 (1997). [https://doi.org/10.1016/S0925-8388\(96\)02721-1](https://doi.org/10.1016/S0925-8388(96)02721-1)
- 15 T. Tsuchida, T. Kan, Synthesis of Al_3BC in air from mechanically activated Al/B/C powder mixtures, *J. Eur. Ceram. Soc.* 19, 1795 (1999). [https://doi.org/10.1016/S0955-2219\(98\)00278-7](https://doi.org/10.1016/S0955-2219(98)00278-7)
- 16 H. M. Hu, E. J. Lavernia, W. C. Harrigan, J. Kajuch, S. R. Nutte, Microstructural investigation on $\text{B}_4\text{C}/\text{Al}-7093$ composite, *Mater. Sci. Eng. A* 297, 94 (2001). [https://doi.org/10.1016/S0921-5093\(00\)01254-5](https://doi.org/10.1016/S0921-5093(00)01254-5)
- 17 M. Kouzele, C. S. Marchi, A. Mortensen, Effect of reaction on the tensile behavior of infiltrated boron carbide–aluminum composites, *Mater. Sci. Eng. A* 337, 264 (2002). [https://doi.org/10.1016/S0921-5093\(02\)00039-4](https://doi.org/10.1016/S0921-5093(02)00039-4)
- 18 M. Kubota, P. Cizek, Synthesis of Al_3BC from mechanically milled and spark plasma sintered Al– MgB_2 composite materials, *J. Alloys Compd.* 457, 209 (2008). <https://doi.org/10.1016/j.jallcom.2007.03.027>
- 19 D. Rena, Q. Denga, J. Wanga, Y. Lia, M. Lia, S. Ranc, S. Dua, Q. Huang, Densification and mechanical properties of pulsed electric current sintered B_4C with in situ synthesized Al_3BC obtained by the molten-salt method, *J. Eur. Ceram. Soc.* 37, 4524 (2017). <https://doi.org/10.1016/j.jeurceramsoc.2017.07.010>
- 20 W. Tian, P. Li, X. Liu, Morphology stability of Al_3BC phase in aluminum alloys, *J. Alloys Compd.* 583, 329 (2014). <https://doi.org/10.1016/j.jallcom.2013.08.205>
- 21 D. C. Halverson, A. J. Pyzik, I. A. Aksay, Processing and Microstructural Characterization of B_4C -Al Cermets, *Ceram. Eng. Sci. Proc.* 6, 736 (1985).
- 22 $ZT = (S^2 \sigma T)/\kappa_{\text{tot}}$ where S , σ , T and κ_{tot} are Seebeck coefficient (also referred as thermopower), electrical conductivity, temperature and total thermal conductivity (sum of the electronic part κ_e and the lattice part κ_{latt}), respectively.
- 23 M. Bouchacourt, F. Thevenot, The correlation between the thermoelectric properties and stoichiometry in the boron carbide phase $\text{B}_4\text{C}-\text{B}_{10.5}\text{C}$, *J. Mater. Sci.* 20, 1237 (1985). <https://doi.org/10.1007/BF01026319>
- 24 G. A. Slack, D. W. Oliver, F. H. Horn, Thermal Conductivity of Boron and Some Boron Compounds, *Phys. Rev. B* 4, 1714 (1971). <https://doi.org/10.1103/PhysRevB.4.1714>

-
- 25 D. G. Cahill, H. E. Fischer, S. K. Watson, R. O. Pohl, G. A. Slack, Thermal properties of boron and borides, *Phys. Rev. B* **40**, 3254 (1989).
<https://doi.org/10.1103/PhysRevB.40.3254>
- 26 T. Mori, Thermal conductivity of a rare-earth B₁₂-icosahedral compound, *Physica B* **383**, 120 (2006). <https://doi.org/10.1016/j.physb.2006.03.072>
- 27 G. Kresse, J. Furthmüller, Efficient iterative schemes for *ab initio* total-energy calculations using a plane-wave basis set, *Phys. Rev. B* **54**, 11169 (1996).
<https://doi.org/10.1103/PhysRevB.54.11169>
- 28 P. Giannozzi, S. De Gironcoli, P. Pavone, S. Baroni, *Ab initio* calculation of phonon dispersions in semiconductors, *Phys. Rev. B* **43**, 7231 (1991).
<https://doi.org/10.1103/PhysRevB.43.7231>
- 29 S. Baroni, P. Giannozzi, A. Testa, Green's-function approach to linear response in solids, *Phys. Rev. Lett.* **58**, 1861 (1987). <https://doi.org/10.1103/PhysRevLett.58.1861>
- 30 J. P. Perdew, K. Burke, M. Ernzerhof, Generalized Gradient Approximation Made Simple, *Phys. Rev. Lett.* **77**, 3865 (1996). <https://doi.org/10.1103/PhysRevLett.77.3865>
- 31 P. E. Blöchl, Projector augmented-wave method, *Phys. Rev. B* **50**, 17953 (1994).
<https://doi.org/10.1103/PhysRevB.50.17953>
- 32 A. Togo, F. Oba, I. Tanaka, First-principles calculations of the ferroelastic transition between rutile-type and CaCl₂-type SiO₂ at high pressures, *Phys. Rev. B* **78**, 134106 (2008). <https://doi.org/10.1103/PhysRevB.78.134106>
- 33 T. J. Scheidemantel, C. Ambrosch-Draxl, T. Thonhauser, J. V. Badding, J. O. Sofo, Transport coefficients from first-principles calculations, *Phys. Rev. B* **68**, 125210 (2003). <https://doi.org/10.1103/PhysRevB.68.125210>
- 34 G. K. H. Madsen, Automated Search for New Thermoelectric Materials: The Case of LiZnSb, *J. Am. Chem. Soc.* **128**, 12140 (2006). <https://doi.org/10.1021/ja062526a>
- 35 G. K. H. Madsen, D. J. Singh, BoltzTraP. A code for calculating band-structure dependent quantities, *Comput. Phys. Commun.* **175**, 67 (2006).
<https://doi.org/10.1016/j.cpc.2006.03.007>
- 36 F. Tran, P. Blaha, Accurate Band Gaps of Semiconductors and Insulators with a Semilocal Exchange-Correlation Potential, *Phys. Rev. Lett.* **102**, 226401 (2009).
<https://doi.org/10.1103/PhysRevLett.102.226401>
- 37 P. Blaha, K. Schwarz, G. K. H. Madsen, D. Kvasnicka, J. Luitz, WIEN2k 14.2, Vienna, Austria (2011).
- 38 S. J. Clark, M. D. Segall, C. J. Pickard, P. J. Hasnip, M. I. J. Probert, K. Refson, M. C. Payne, First principles methods using CASTEP, *Z. Krist.* **220**, 567 (2005).
<https://doi.org/10.1524/zkri.220.5.567.65075>
- 39 J. P. Perdew, A. Ruzsinszky, G. I. Csonka, O. A. Vydrov, G. E. Scuseria, L. A. Constantin, X. Zhou, K. Burke, Restoring the Density-Gradient Expansion for

-
- Exchange in Solids and Surfaces, *Phys. Rev. Lett.* **100**, 136406 (2008).
<https://doi.org/10.1103/PhysRevLett.100.136406>
- 40 M. Christensen, A. B. Abrahamsen, N. B. Christensen, F. Juranyi, N. H. Andersen, K. Lefmann, J. Andreasson, C. R. H. Bahl, B. B. Iversen, Avoided crossing of rattler modes in thermoelectric materials, *Nat. Mater.* **7**, 811 (2008).
<https://doi.org/10.1038/nmat2273>
- 41 D. Volja, B. Kozinsky, A. Li, D. Wee, N. Marzari, M. Fornari, Electronic, vibrational, and transport properties of pnictogen-substituted ternary skutterudites, *Phys. Rev. B* **85**, 245211 (2012). <https://doi.org/10.1103/PhysRevB.85.245211>
- 42 D. Wee, B. Kozinsky, M. Fornari, Frequency of Filler Vibrations in CoSb₃ Skutterudites: A Mechanical Interpretation, *J. Phys. Soc. Japan* **82**, 014602 (2013).
<https://doi.org/10.7566/JPSJ.82.014602>
- 43 C. Bourgès, Y. Bouyrie, A. R. Supka, R. Al Rahal Al Orabi, P. Lemoine, O. I. Lebedev, M. Ohta, K. Suekuni, V. Nassif, V. Hardy, R. Daou, Y. Miyazaki, M. Fornari, E. Guilmeau, High-Performance Thermoelectric Bulk Colusite by Process Controlled Structural Disordering, *J. Am. Chem. Soc.* **140**, 2186 (2018).
<https://doi.org/10.1021/jacs.7b11224>
- 44 V. Pavan Kumar, A. R. Supka, P. Lemoine, O. I. Lebedev, B. Raveau, K. Suekuni, V. Nassif, R. Al Rahal Al Orabi, M. Fornari, E. Guilmeau, High Power Factors of Thermoelectric Colusites Cu₂₆T₂Ge₆S₃₂ ($T = \text{Cr, Mo, W}$): Toward Functionalization of the Conductive “Cu–S” Network, *Adv. Energy Mater.* **9**, 1803249 (2018).
<https://doi.org/10.1002/aenm.201803249>
- 45 R. Al Rahal Al Orabi, E. Orisakwe, D. Wee, B. Fontaine, R. Gautier, J.-F. Halet, M. Fornari, Prediction of high thermoelectric potential in AMN₂ layered nitrides: electronic structure, phonons, and anharmonic effects, *J. Mater. Chem. A* **3**, 9945 (2015).
<https://doi.org/10.1039/c5ta00546a>
- 46 P. Vaqueiro, R. Al Rahal Al Orabi, S. D. N. Luu, G. Guélou, A. V. Powell, R. I. Smith, J.-P. Song, D. Wee, M. Fornari, The role of copper in the thermal conductivity of thermoelectric oxychalcogenides: do lone pairs matter?, *Phys. Chem. Chem. Phys.* **17**, 31735 (2015). <https://doi.org/10.1039/C5CP06192J>
- 47 D. T. Morelli, V. Jovovic, J. P. Heremans, Intrinsically Minimal Thermal Conductivity in Cubic I–V–VI₂ Semiconductors, *Phys. Rev. Lett.* **101**, 035901 (2008).
<https://doi.org/10.1103/PhysRevLett.101.035901>
- 48 P. Debye, Zur Theorie der spezifischen Wärmen, *Ann. Phys.* **344**, 789 (1912).
<https://doi.org/10.1002/andp.19123441404>
- 49 G. A. Slack, Nonmetallic crystals with high thermal conductivity, *J. Phys. Chem. Solids* **34**, 321 (1973). [https://doi.org/10.1016/0022-3697\(73\)90092-9](https://doi.org/10.1016/0022-3697(73)90092-9)
- 50 R. Al Rahal Al Orabi, J. Hwang, C.-C. Lin, R. Gautier, B. Fontaine, W. Kim, J.-S. Rhyee, D. Wee, M. Fornari, Ultralow Lattice Thermal Conductivity and Enhanced Thermoelectric Performance in SnTe:Ga Materials, *Chem. Mater.* **29**, 612 (2017).
<https://doi.org/10.1021/acs.chemmater.6b04076>

-
- 51 R. Al Rahal Al Orabi, N. A. Mecholsky, J. Hwang, W. Kim, J. Rhyee, D. Wee, M. Fornari, Band Degeneracy, Low Thermal Conductivity, and High Thermoelectric Figure of Merit in SnTe–CaTe Alloys, *Chem. Mater.* 28, 376 (2016).
<https://doi.org/10.1021/acs.chemmater.5b04365>